Carrier lifetimes and threshold currents in HgCdTe double heterostructure and multiquantum-well lasers

Y. Jiang, M. C. Teich, and W. I. Wang
Department of Electrical Engineering, Columbia University, New York, New York 10027

(Received 2 November 1990; accepted for publication 14 January 1991)

The Auger and radiative combination carrier lifetimes in HgCdTe bulk and quantum-well structures, with band gaps in the wavelength range 2–5 μm, are calculated. The Auger recombination rate in a HgCdTe quantum well (QW) is shown to be significantly smaller than that in bulk material. Threshold current densities of HgCdTe double-heterostructure (DH) and multiquantum-well (MQW) lasers are calculated. In a HgCdTe DH laser, Auger recombination dominates the carrier loss at threshold. In a HgCdTe MQW laser, on the other hand, radiative recombination dominates the carrier loss. MQW lasers shown improved temperature performance over conventional DH lasers.

I. INTRODUCTION

There has been increasing interest in developing semiconductor lasers that operate in the 2–5 μm wavelength range.[1,2] These lasers have found application in high-resolution gas spectroscope, air-pollution monitoring, and infrared heterodyne detection.[1] They have potential applications in communication systems utilizing fluoride glass fibers,[3] which have minimal losses in the 2–4 μm wavelength region. The intrinsic losses in glass fibers arise from Rayleigh scattering, which decreases as $1/\lambda^4$ as the wavelength increases.[4] With highly developed fluoride glass fibers the transmission losses in a communication system can be substantially reduced, and efficient lasers operating in this wavelength range would be required.

Narrow-gap III-V semiconductor systems, such as InGaAsSb/AlGaAsSb, InAsPSb/GaSb, and InAsPSb/InAs are the candidates for lasers operating in this wavelength range and, indeed, lasing at low temperatures has been observed in these materials. There has also been progress in growing lasers of materials with a certain degree of lattice mismatch, such as InAsSb/GaSb.[5] However, the fact that the index of reflection of GaSb is larger than that of InAsSb makes it impossible to realize optimal design in these lasers. The steep increase of threshold current with temperature in these III-V lasers indicates that the dominant carrier losses are due to Auger recombination; improvement is not likely with the use of novel configurations, such as quantum-well structures.[6] It is known that for lasers in which Auger recombination dominates the carrier losses, the threshold current for achieving lasing increases and the internal quantum efficiency decreases so rapidly with temperature that they cannot lase at relatively high temperatures.

Another candidate material for lasers in this wavelength range is HgCdTe. However, it also exhibits a large Auger recombination carrier loss. Indeed, lasing is achieved in HgCdTe lasers only at temperatures much lower than room temperature with optical pumping.[3,7] On the other hand, the lattice mismatch between HgTe is well and CdTe is as small as 0.3%, so that HgCdTe is well-lattice-matched to CdTe for a large range of Hg composition. Moreover, recent advances in growing HgCdTe quantum-well structures[8] opens the possibility of making HgCdTe quantum-well lasers,[9] which are expected to have reduced Auger recombination loss and may be operated in room temperature with current injection.

In Secs. II and III we calculate and compare the Auger recombination lifetimes and radiation recombination lifetimes in HgCdTe bulk and quantum-well structures. In Sec. IV we compare the threshold currents in HgCdTe double heterostructure (DH) and multiquantum-well (MQW) lasers.

II. AUGER RECOMBINATION

A. CCCH Auger recombination in bulk material

Band-to-band Auger recombination in narrow-gap HgCdTe is dominated by the CCCH process,[10,11] in which, as shown in Fig. 1, a conduction-band electron 1 (C) recombines with a heavy hole 1′ (H) and excites an electron 2 (C) to the state 2′ (C)of higher energy.

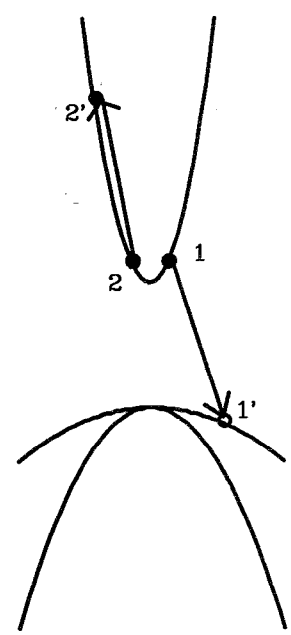

FIG. 1. The CCCH Auger process.

 0021-8979/91/106869-07$03.00

The CCCH Auger recombination rate R ($\mathrm{cm}^{-3}\,\mathrm{sec}^{-1}$) is[12,13]

$$R_{\mathrm{Aug}}=\frac{2\pi}{\hbar}\left(\frac{1}{8\pi^3}\right)^3\int\int\int\int d^3k_1 d^3k_2 d^3k_{1'} d^3k_{2'}|M_A|^2 P \times(1,1',2,2')\delta(\mathbf{k}_1+\mathbf{k}_2-\mathbf{k}_{1'}-\mathbf{k}_{2'})\delta(E_i-E_f), \tag{1}$$

where the k's are carrier wavevectors, E_i and E_f are the initial and final energies of the process, respectively, and

$$E_i-E_f=E(1')+E(2')-E(1)-E(2). \tag{2}$$

Neglecting exchange terms, the matrix element is

$$|M_A|^2=4\left(\frac{4\pi q^2}{\epsilon}\right)^2\left|\frac{F_{1,1'}F_{2,2'}}{(\mathbf{k}_{2'}-\mathbf{k}_2)^2+\lambda^2}\right|^2, \tag{3}$$

where q, ϵ, and λ are the electron charge, dielectric constant, and screening factor, respectively, and $|F_{ij}|^2$ are the overlap functions.[14] The quantity $P(1,1',2,2')$, taking the reverse process of CCCH Auger recombination into account also, represents the occupation probabilities. Assuming that the electron and hole distributions f_n and f_p can be expressed as Fermi distributions, with electron and hole equilibrium Fermi levels F_n and F_p, respectively, we have

$$\begin{aligned}P(1,1',2,2')&=f_n(\mathbf{k}_1)\,f_n(\mathbf{k}_2)\,f_p(\mathbf{k}_{1'})[1-f_n(\mathbf{k}_{2'})]\\&\quad-[1-f_n(\mathbf{k}_1)][1-f_n(\mathbf{k}_2)]\\&\quad\times[1-f_p(\mathbf{k}_{1'})]f_n(\mathbf{k}_{2'})\\&=\{1-\exp[-(F_n-F_p)/k_BT]\}f_n(\mathbf{k}_1)\\&\quad\times f_n(\mathbf{k}_2)f_p(\mathbf{k}_{1'})[1-f_n(\mathbf{k}_{2'})],\end{aligned} \tag{4}$$

where k_B is the Boltzmann constant and T is the temperature. Since the energy of the excited electron is sufficiently high so that $E_{2'}-F_n \gg kT$, $f_n(\mathbf{k}_{2'})$ in (4) can be taken as zero. When $P(1,1',2,2')$ is positive the Auger recombination process dominates, whereas when $P(1,1',2,2')$ is negative the reverse process, impact ionization process, dominates.

Although the integrations in Eq. (1) extend over all values of the wavevectors, they are actually limited by the conservation of energy and momentum. The lowest permissible value of the excited electron energy $E_{2'}$ is called the threshold energy of the Auger recombination. $P(1,1',2,2')$ is maximum at the threshold.

The threshold energy of the CCCH process in HgCdTe lies high in the conduction band, where it is not parabolic. One method in dealing with the nonparabolic band-bending is provided by Landsberg and Yu.[15] Although the parabolic-band approximation introduces errors in the absolute values of the calculated recombination rates, it is good enough for our purposes to compare the Auger recombination rate in HgCdTe bulk and that in quantum-well structures. We assume that the conduction-band electron and heavy-hole effective masses are m_c and m_h, respectively. Defining the new variables

$$\mathbf{h}=\mathbf{k}_1+\mathbf{k}_2=\mathbf{k}_{1'}+\mathbf{k}_2', \tag{5}$$

$$\mathbf{j}=\mathbf{k}_2-\mathbf{k}_1, \tag{6}$$

and

$$\mathbf{K}=\mathbf{k}_{1'}-\frac{\mathbf{h}}{(1-m_c/m_h)}, \tag{7}$$

simplifies the integration in Eq. (1). The δ functions for momentum and energy conservation reduce the twelfth-order integration in Eq. (1) to eighth order. F_{22}, can be taken as unity.[11,12] Because k_2, is large at the threshold, and the Auger recombination arises principally from carriers near the threshold, the matrix element $|M_A|$ can be taken as constant. Further analysis reduces the integration in Eq. (1) to a third-order one, which can be calculated numerically.[6]

If the Fermi levels are sufficiently away from the band edges, Eq. (1) can be approximated as

$$R_{\mathrm{Aug}}=Cpn^2, \tag{8}$$

where n and p are the electron and hole concentrations, respectively, and the constant C is called the Auger recombination constant. For intrinsic semiconductors, and for semiconductors with high levels of carrier injection, which is the case in semiconductor lasers, $n=p$. The Auger recombination lifetime, defined as

$$\tau=p/R_{\mathrm{Aug}}, \tag{9}$$

is a measure that is often used to characterize the performance of semiconductor lasers.

Figure 2 shows the calculated Auger recombination lifetime in bulk $Hg_{0.578}Cd_{0.422}Te$ at various values of the temperature. The band gap of HgCdTe is calculated from the results given in Ref. 16, as are the effective masses of the electron, light, and heavy holes. Figure 2 shows that, at low carrier concentrations, $1/\tau \propto n^2$.

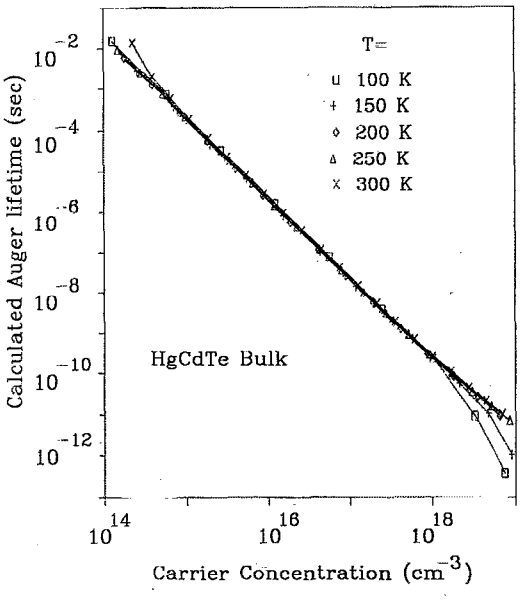

FIG. 2. Calculated Auger recombination lifetime in bulk $Hg_{0.578}Cd_{0.422}Te$ at various values of the temperature.

B. CCCH Auger recombination in a quantum well

The states of the carriers in the ith band of a quantum well of width d with infinite barriers can be written as[17]

$$\phi_{i,m}=u_{i,\mathbf{k}}(\mathbf{r}_t)e^{i\mathbf{k}\mathbf{r}_t}\sqrt{(2/d)}\sin(\xi_m z), \tag{10}$$

where u is the periodic part of the Bloch function, $\mathbf{k}$ and $\mathbf{r}_t$ are two-dimensional vectors perpendicular to the width of the well, and

$$\xi_m = m\frac{\pi}{d}, \quad m = 1,2,\ldots . \tag{11}$$

In analogy with the three-dimensional expression given in Eq. (1), the two-dimensional CCCH Auger recombination rate per unit volume is

$$R_{\mathrm{Aug}}=\frac{2\pi}{\hbar}\left(\frac{1}{4\pi^2}\right)^3\frac{1}{d^3}\sum_{\xi,\xi_1,\xi_{1'},\xi_2,\xi_{2'}}\int\int\int\int d^2k_1 d^2k_2 d^2 \times k_{1'}d^2k_{2'}|M_A|^2 p(1,1',2,2') \times\delta(\mathbf{k}_1+\mathbf{k}_2-\mathbf{k}_{1'}-\mathbf{k}_{2'})\delta(E_i-E_f). \tag{12}$$

However, unlike the case of bulk material, the matrix element is now

$$|M_A|^2=4\left(\frac{4\pi g^2}{\epsilon}\right)^2\left|\frac{F_{1,1'}F_{2,2'}G_{1,1'}(\xi)G_{2,2'}(-\xi)}{(\mathbf{k}_{2'}-\mathbf{k}_2)^2+\xi^2+\lambda^2}\right|^2, \tag{13}$$

where

$$G_{i,j}(\xi)=\tfrac{1}{2}(\delta_{\xi,\xi_i-\xi_j}+\delta_{\xi,\xi_j-\xi_i}-\delta_{\xi,\xi_i+\xi_j}-\delta_{\xi,-\xi_i-\xi_j}). \tag{14}$$

The integrals over the k_z's in Eq. (1) for the bulk material become summations over the ξ's for the quantum-well structures. The $G_{ij}(\xi)$'s impose selection rules on the summations. Equation (12) can also be reduced to a third-order integration as described in Sec. II A.

As shown in Fig. 3, the Auger recombination lifetime in a HgCdTe QW is increased substantially over that of the bulk material. Certainly, the increase of the effective band gap in the quantum-well structure increases the Auger lifetime, but it is not the major factor in the increase. Indeed, Fig. 3 shows that the Auger lifetime in a $Hg_{0.7}Cd_{0.3}Te$ quantum well is longer than that in bulk $Hg_{0.578}Cd_{0.422}Te$, while the former has an effective band gap that is smaller than the latter. This demonstrates that the increase of Auger lifetime in a quantum-well structure is mostly due to the reduction of dimensions to two. Figure 3 also demonstrates the trend of increasing Auger lifetime with decreasing well width.

Figure 4 shows the Auger lifetime in a HgCdTe quantum well of $d = 200$ Å at various values of the temperature. At low carrier concentrations, $1/\tau \propto n^2$.

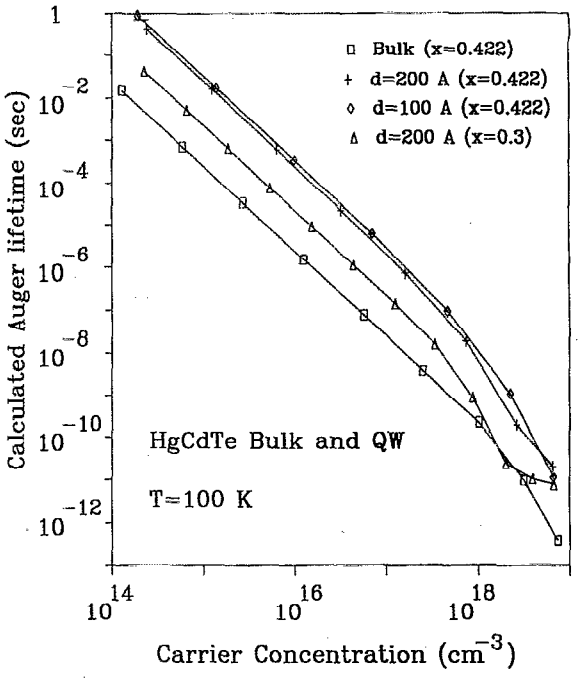

FIG. 3. Calculated Auger recombination lifetime in $Hg_{1-x}Cd_xTe$ bulk and quantum-well structures at $T = 100$ K.

III. RADIATIVE RECOMBINATION

Spontaneous radiation in a semiconductor laser arises from radiative recombination. The radiative recombination rate ($cm^{-3}\,s^{-1}$) in bulk material is

$$R_{\mathrm{rad}}=\frac{2\pi}{\hbar}\sum_{v=l,h}\frac{2}{8\pi^3}\int\int\int d^3k_c d^3k_v dE\rho(E)|H_{if}|^2 P \times(E_c,E_v)\delta(\mathbf{k}_c-\mathbf{k}_v)\delta(E_c-E_v-E), \tag{15}$$

where E and $\rho(E)$ are the photon energy and density of states, k_i and E_i are the wave vectors and energies of the carriers, and $P(E_c,E_v)$ is the joint distribution of electrons and holes. We consider radiative transitions from the conduction band (c) to the heavy-hole band (h) and light-

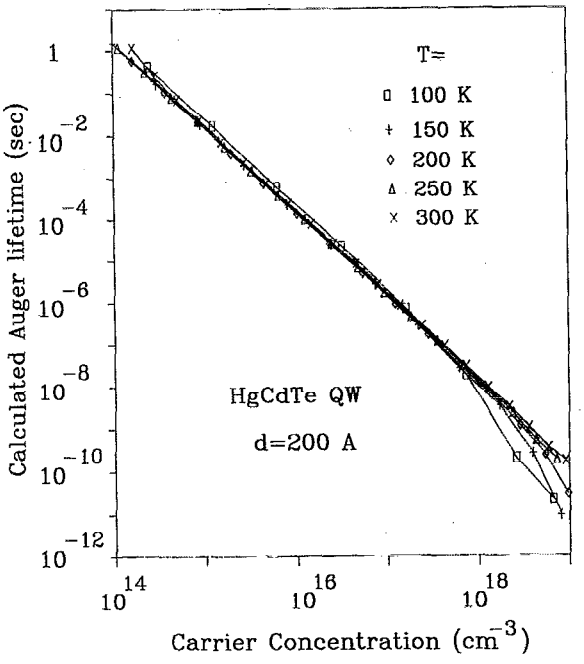

FIG. 4. Calculated Auger recombination lifetime in a $Hg_{0.578}Cd_{0.422}Te$ quantum well of 200 Å well width at various temperatures.

hole band (l), i.e., $\nu = l,h$. The matrix element for spontaneous emission can be written as

$$|H_{if}| = \frac{q}{m}|\langle 1|\mathbf{A}|0\rangle \cdot \langle k_v|\mathbf{p}|k_c\rangle| = \frac{q}{m}|\langle 1|\mathbf{A}|0\rangle| \cdot |M_r|, \tag{16}$$

where $\mathbf{A}$ is the vector potential of the radiation field, and

$$|M_r| = |\langle k_v|\mathbf{p}\cdot\hat{e}\,|k_c\rangle| \tag{17}$$

is the momentum matrix element along the direction of the vector potential ($\hat{e}$ is the unit vector in that direction).

With the assumption of parabolic bands, Eq. (15) becomes[18]

$$R_{\rm rad} = \frac{2nq^2|M_r|^2}{\pi m_0^2 \epsilon_0 h^2 c^3} \sum_{v=l,h} \left[\frac{\hbar^2}{2}\left(\frac{1}{m_c}+\frac{1}{m_c}\right)\right]^{-3/2} \times \int_{E_g}^{\infty} dE\, E(E-E_g)^{1/2} f_n(E_c) f_p(E_v), \tag{18}$$

where ϵ is the dielectric constant of free space, n is the refractive index of the active layer, m_0 is the free electron mass, and E_g is the band-gap energy.

According to the Kane model,[19] the momentum matrix element can be written as

$$|M_r|^2 = \frac{m_0^2 E_g(E_g+\Delta)}{12 m_c (E_g + 2\Delta/3)}, \tag{19}$$

where Δ is the spin-splitoff gap energy.

In analogy with Eqs. (15) and (18), the radiative recombination rate in a quantum well is[18]

$$R_{\rm rad} = \frac{2\pi}{\hbar} \sum_{v=l,h} \int\int\int d^2k_c d^2k_v\, dE \rho(E) |H_{if}|^2 P \times (E_c,E_v)\delta(\mathbf{k}_c - \mathbf{k}_v)\delta(E_c - E_v - E), \tag{20}$$

$$= \frac{4\pi n q^2 |M_r|^2}{d m_0^2 \epsilon_0 h^2 c^3} \sum_{v=l,h} \left[\frac{\hbar^2}{2}\left(\frac{1}{m_c}+\frac{1}{m_v}\right)\right]^{-1} \times \int_{E_g}^{\infty} dE\, E f_n(E_c) f_p(E_v). \tag{21}$$

Figure 5 shows the radiative lifetime in HgCdTe bulk and QW structures as a function of carrier concentration. At low carrier concentrations, $1/\tau_r \propto n$. Figures 6 and 7 show the behavior of the spontaneous recombination lifetimes in $Hg_{0.578}Cd_{0.422}Te$ bulk and in a QW of width 100 Å, respectively, at various values of the temperature. The radiative recombination lifetime is substantially shorter in the QW structure, while the Auger recombination lifetime is longer, as shown earlier.

IV. THRESHOLD CURRENT

The lasing condition for a single-mode semiconductor laser of cavity length L is[18,20]

$$g\Gamma = \alpha_a + \frac{1}{2L}\ln\left(\frac{1}{R_1 R_2}\right), \tag{22}$$

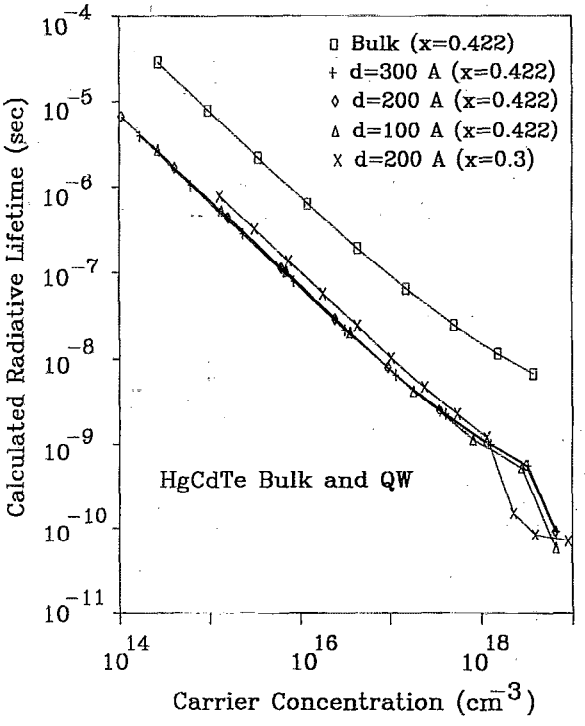

FIG. 5. Calculated radiative recombination lifetime in $Hg_{1-x}Cd_xTe$ bulk and quantum-well structures at $T = 100$ K.

where g is the gain coefficient of the lasing mode, Γ is the optical confinement factor, α_a is the average absorption coefficient in the cladding and active layers, excluding the absorption due to carriers, and R_i are the coefficients of

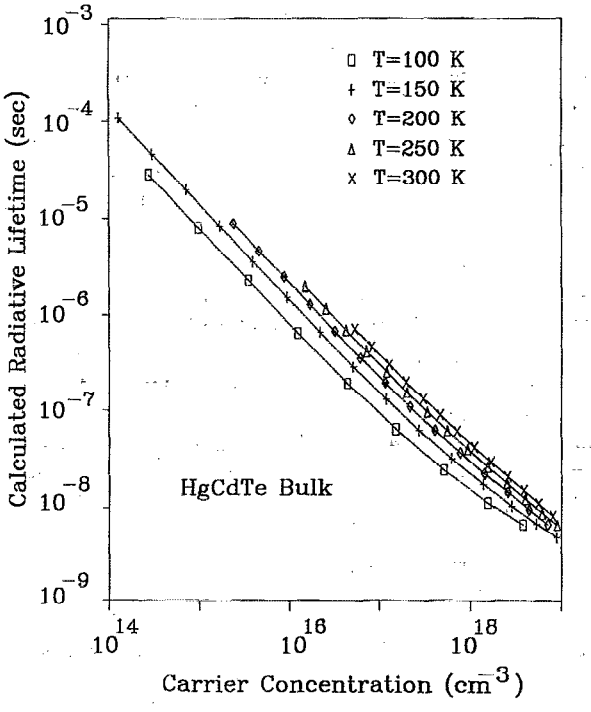

FIG. 6. Calculated radiative recombination lifetime in bulk $Hg_{0.578}Cd_{0.422}Te$ at various values of the temperature.

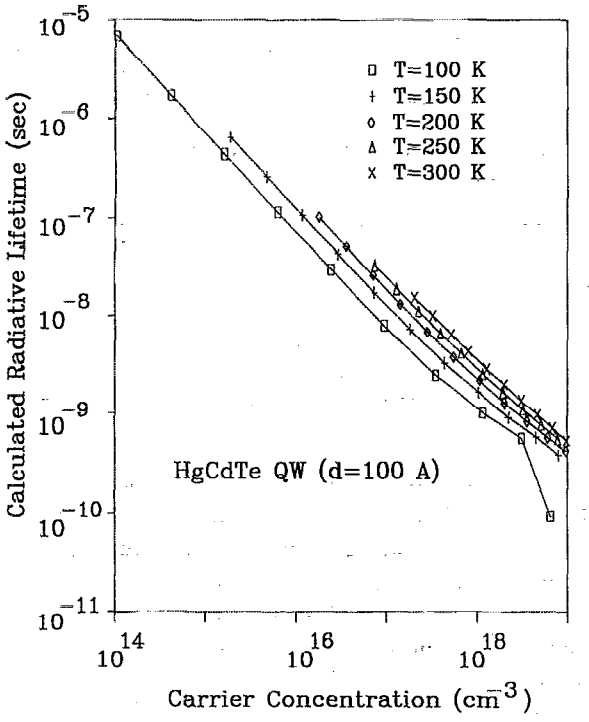

FIG. 7. Calculated radiative recombination lifetime in a $Hg_{0.578}Cd_{0.422}Te$ quantum well of 100 Å well width at various values of the temperature.

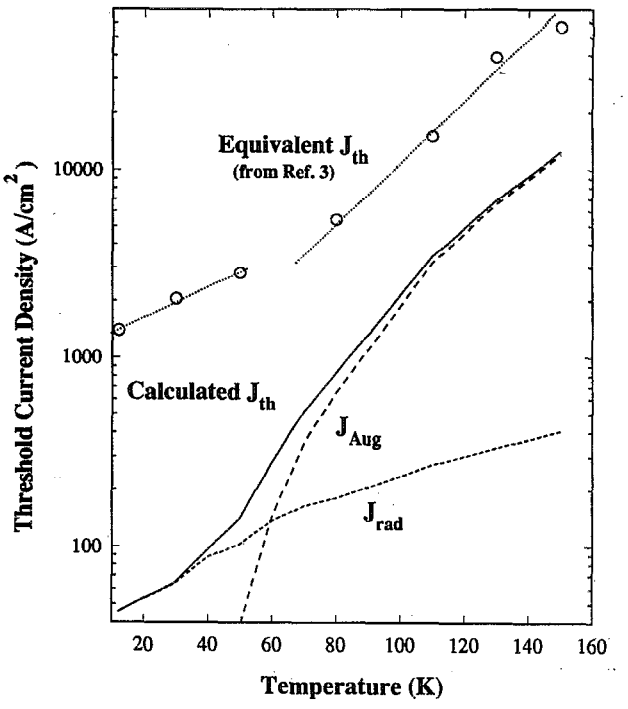

FIG. 8. Comparison of the calculated threshold current density and the threshold current density from the experiment reported in Ref. 3 at various temperatures for the laser structure discussed in Ref. 3. The calculated threshold current density J_{th} is the sum of the calculated Auger recombination current J_{Aug} and radiative recombination current J_{rad} $\alpha_a = 15\ cm^{-1}$ and $R_1 = R_2 = 0.32$ are assumed in the calculation. The calculated fundamental mode threshold current density is lower than the observed multimode equivalent threshold current density, but the variation of the calculated threshold current density with temperature resembles the observed one.

reflection at the two facets. We assume in our calculation that $\alpha_a = 15\ cm^{-1}$ and $R_1 = R_2 = 0.32$.

For a single-mode double heterostructure laser, the gain spectrum is[18,20]

$$g(E) = \frac{q^2 h |M_r|^2}{4\pi^2 \epsilon_0 n c m_0^2 C} \sum_{v=h,l} \left[\frac{\hbar^2}{2}\left(\frac{1}{m_c} + \frac{1}{m_v}\right)\right]^{-3/2} \times \frac{(E - E_g)^{1/2}}{E} [f_n(E_c) + f_p(E_v) - 1]. \quad (23)$$

For a quantum-well laser the gain spectrum is[18,20]

$$g(E) = \frac{2\pi q^2 |M_r|^2}{\epsilon_0 n c h m_0^2} \frac{1}{E} \sum_{v=h,l} \left(\frac{1}{m_c} + \frac{1}{m_v}\right)^{-1} \times [f_n(E_c) + f_p(E_v) - 1]. \quad (24)$$

At low carrier concentrations, where $f_n(E_c)$ and $f_p(E_v)$ are small, the gain coefficient is negative, and the material acts as an absorber. The gain coefficient increases with increasing carrier concentration; when it becomes large enough to satisfy the condition in Eq. (22), the laser threshold is reached. The corresponding carrier concentration and injection current density are called the threshold carrier concentration and the threshold current density J_{th}, respectively. The threshold current density is the sum of the rates of the carrier loss per unit area at the threshold carrier concentration.

$$J_{th} = q d_{active}(R_{rad} + R_{Aug} + R') = J_{rad} + J_{Aug} + J', \quad (25)$$

where d_{active} is the active layer thickness. R' is the sum of the rates of all the other nonradiative carrier losses, such as loss due to material defects, excluding the Auger recombination loss. J_{rad}, J_{Aug}, and J' are the current densities due to the spontaneous radiative recombination, the Auger recombination, and other nonradiative recombination mechanisms, respectively. We neglect R' and J' in our calculation.

As an empirical rule, the threshold current density of a semiconductor laser varies roughly exponentially with the temperature, $J_{th} \propto \exp(T/T_0)$, over a certain range of temperature. T_0 is called the characteristic temperature and is a measure that is often used to characterize the temperature performance of semiconductor lasers.

A recent experiment[3] was conducted with an optically pumped HgCdTe/CdTe laser with an active layer consisting of 4 μm of $Hg_{0.578}Cd_{0.422}Te$, which supports about seven transverse modes. Stimulated emission was observed up to 150 K at a wavelength 2.9 μm, with an equivalent threshold current density of 56 kA/cm^2 at 150 K. Figure 8 shows equivalent threshold current density calculated from the observed threshold optical power P_{th}, from Ref. 3 and the calculated fundamental mode threshold current density J_{th} at various values of the temperature. The fundamental mode threshold current density is obviously lower than the

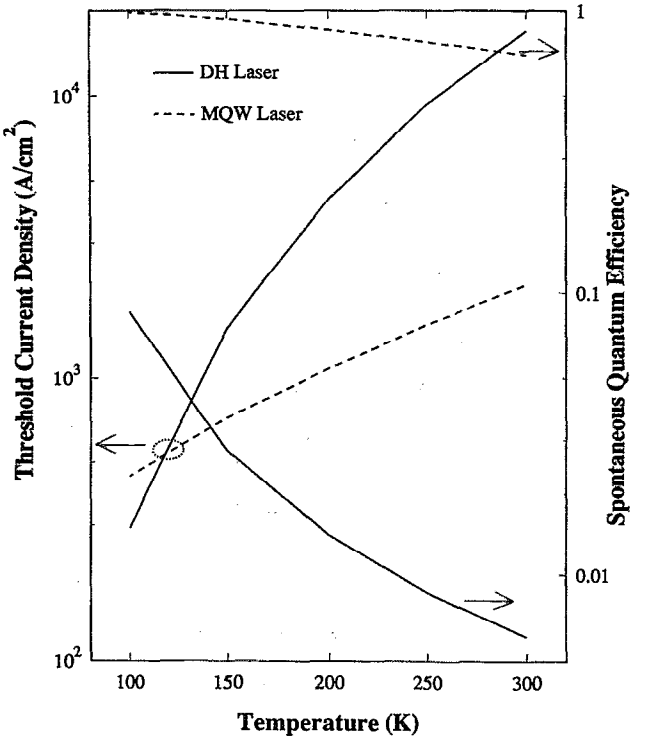

FIG. 9. Calculated threshold current densities and spontaneous quantum efficiency of a $Hg_{0.578}Cd_{0.422}Te$ DH laser with $d_{active} = 0.3$ μm and a 15 period $Hg_{0.578}Cd_{0.422}Te$/CdTe(100 Å/100 Å) MQW laser, at various values of the temperature.

observed multimode equivalent threshold current density, but the variation of the calculated threshold current density with temperature resembles the observed threshold optical power. The calculated values of J_{Aug} and J_{rad} are also shown in Fig. 8. We can see that the threshold current density is dominated by the Auger recombination current at 80 K and above, and is dominated by the radiation recombination current at 50 K and below. The value of J_{Aug} increases with temperature drastically, whereas J_{rad}, on the other hand, only increases mildly with temperature. Therefore, above 50 K, the threshold current density increases drastically with temperature so that T_0 is small, whereas below 50 K, the threshold current density increases mildly with temperature so that T_0 is larger.

In order to achieve single-transverse-mode lasing, the active layer of a HgCdTe DH laser oscillating at 2.9 μm wavelength must be 0.5 μm or thinner. On the other hand, a very thin active layer, such as a single quantum well, provides very limited optical confinement at wavelengths longer than 2 μm so that it may be hard to achieve lasing. Figure 9 shows the calculated threshold current densities of a DH laser with a 0.3 + μm active layer, and a 15-period $Hg_{0.578}Cd_{0.422}Te$/CdTe (100/100 Å) MQW laser, at various values of the temperature. The spontaneous quantum efficiency, which is defined as[17]

$$\eta = R_{rad}/(R_{rad} + R_{Aug}), \tag{26}$$

is also shown in Fig. 9.

TABLE I. Calculated threshold current density at 100 K for $Hg_{0.578}Cd_{0.422}Te$/CdTe DH and MQW lasers with various values of the well thickness. Because the calculation was carried out for a low temperature ($T = 100$ K) the threshold current density is lower for the bulk laser.

Individual well thickness (Å)	Number of wells	Threshold current density (A/cm²)
100	15	445
150	12	418
200	10	500
250	8	794
300	7	603
Bulk ($d_{active} = 0.3$ μm)	DH	293

Auger recombination dominates the threshold current density in the DH laser. The spontaneous quantum efficiency η is therefore small, and the threshold current increases rapidly with temperature, with a characteristic temperature T_0 as low as 50 K. This device is unable to lase at relative high temperatures. In contrast, radiative recombination dominates the threshold current density in the MQW laser. The spontaneous quantum efficiency is substantially larger, and the threshold current density does not increase as rapidly with temperature as in the DH laser. The characteristic temperature T_0 is 127 K, which is quite a bit larger than that for the DH laser and is in the same range as that for GaAs lasers. Thus, an MQW HgCdTe laser may achieve lasing at room temperature with current injection.

Table I shows the calculated threshold current densities at 100 K for a DH laser and an MQW laser with various values of the well thickness. The width of the barriers of the MQW's are all 100 Å, and the active layers are all about 0.3 μm in overall thickness. The MQW laser of well width 150 Å appears to achieve the lowest threshold current density among the MQW lasers at 100 K.

V. CONCLUSION

We conclude that the two-dimensional behavior of HgCdTe/CdTe quantum-well structures reduces the Auger recombination rate significantly from that of bulk material. As a consequence, the Auger recombination current in a HgCdTe MQW laser is reduced below the radiative recombination current at threshold. This increases the characteristic temperature and spontaneous quantum efficiency, and therefore the possibility of achieving room-temperature lasing in HgCdTe MQW devices.

ACKNOWLEDGMENTS

This work was supported by the Center for Telecommunications Research, the Joint Services Electronics Program (DAAL 03-88-C-0009) and the Naval Research Laboratory (N00014-89-K-2020). We are grateful to Faige Singer and Jull Hacker for useful suggestions.

[1] Y. Horikoshi, in *Semiconductors and Semimetals*, edited by W. T. Tsang (Academic, New York, 1985), Vol. 22C, Ch. 3.
[2] D. L. Partin, IEEE J. Quantum Electron. **QE-24**, 1716 (1988).

[3] A. Ravid, A. Zussman, G. Cinader, and A. Oron, Appl. Phys. Lett. **55**, 2704 (1989).
[4] W. T. Tsang and N. A. Olsson, Appl. Phys. Lett. **43**, 8 (1983).
[5] J. P. van der Ziel, T. H. Chiu, and W. T. Tsang, Appl. Phys. Lett. **47**, 1139 (1985); J. P. van der Ziel, T. H. Chiu, and W. T. Tsang, Appl. Phys. Lett. **48**, 315 (1986).
[6] Y. Jiang, M. C. Teich, and W. I. Wang, J. Appl. Phys. **69**, 836 (1991).
[7] T. C.Harman, J. Electron. Mater. **8**, 191 (1979).
[8] R. D. Feldman, C. L. Cesar, M. N. Islam, R. F. Austin, A. E. DiGiovanni, and J. Shah, J. Vac. Sci. Technol. A **7**, 431 (1989).
[9] R. A. Reynolds, J. Vac. Sci. Technol. A **7**, 269 (1989).
[10] R. R. Gerhardts, R. Dornhaus, and G. Nimtz, Solid-State Electron. **21**, 1467 (1978).
[11] P. E. Peterson, in *Semiconductors and Semimetals,* edited by R. K. Willardson and A. C. Beer (Academic, New York, 1981), Vol. 18, Ch. 4.
[12] A. Haug, Appl. Phys. Lett. **42**, 512 (1983).
[13] M. Takeshima, Phys. Rev. B **25**, 5390 (1982).
[14] A. R. Beatie and P. T. Landsberg, Proc. R. Soc. A **249**, 16 (1959).
[15] P. T. Landsberg and Y. J. Yu, J. Appl. Phys. **63**, 1789 (1988).
[16] W. M. Higgins, G. N. Pultz, R. G. Roy, R. A. Lancaster, and J. L. Schmit, J. Vac. Sci. Technol. A **7**, 271 (1989).
[17] A. Sugimura, IEEE J. Quantum Electron. **QE-19**, 932 (1983).
[18] G. P. Agrawal and N. K. Dutta, *Long-Wavelength Semiconductor Lasers* (Van Nostrand Reinhold Company, New York, 1986).
[19] E. O. Kane, J. Phys. Chem. Solids **1**, 249 (1957).
[20] A. Yariv, *Quantum Electronics,* 3rd. ed. (Wiley, New York, 1989).